International Journal of
Mathematical Modelling & Computations
Vol. 02, No. 01, 2012, 1 - 19

Dual Boundary Element Analysis of Cracked Plates

A. Portela*

Universidade de Évora, Escola de Ciências e Tecnologia, 7004-516 Évora, Portugal.

Received: 11 June 2011; Accepted: 21 December 2011.

Abstract. The dual boundary element method is formulated for the analysis of linear elastic cracked plates. The dual boundary integral equations of the method are the displacement and the traction equations. When these equations are simultaneously applied along the crack boundaries, general crack problems can be solved in a single-region formulation, with both crack boundaries discretized with discontinuous boundary elements. The stress intensity factors evaluation is carried out by the J-integral decomposition method which is applied on a circular path, defined around each crack tip. Examples of geometries with edge, and embedded cracks are analyzed. The accuracy and efficiency of the dual boundary element method and the J-integral make the present formulation ideal for the study of cracked plates.

Keywords: Dual boundary integral equations, Crack modelling, Computation of principal-value integral, General-shape discontinuous elements.

Index to information contained in this paper

1. Introduction

The boundary element method is a well established numerical technique in the engineering community, see Brebbia and Dominguez [2]. Its formulation in elastostatics is based on the displacement boundary integral equation which is rooted in the classical work theorem, see Portela [26]. The boundary element method has been successfully applied to linear elastic problems in domains containing no degenerated geometries. These degeneracies, either internal or edge surfaces which include no area or volume and across which the displacement field is discontinuous, are defined as mathematical cracks. For symmetric crack problems only one side

*Corresponding author. Email: aportela@uevora.pt

of the crack need be modelled and a single-region boundary element analysis may be used. However, the solution of general crack problems cannot be achieved in a single-region analysis with the direct application of the boundary element method, because the coincidence of the crack boundaries gives rise to an ill-conditioned problem. The equations for a point located at one of the boundaries of the crack are identical to those equations for the point with the same coordinates but on the opposite surface, because the same integral equation is collocated with the same integration path, at both coincident points.

Some special techniques have been devised to overcome this difficulty. Among these, the most important are: the crack Green's function method, Snyder and Cruse [32]; the displacement discontinuity method, Crouch [6]; the subregions method, Blandford, Ingraffea and Liggett [1]; and the dual boundary element method, Portela, Aliabadi and Rooke [28]. The crack Green's function method which eliminates the need for discretization of the crack, is limited to problems with a single straight traction-free crack. In the displacement discontinuity method, where the cracks are modelled by a single line of elements, new variables are introduced into the boundary integrals, see Sladek, Sladek and Balas [31] and Cruse [7]. The subregions method introduces artificial boundaries into the body which connect the cracks to the boundary in such a way that the domain is divided into subregions without cracks. The main drawback of this method is that the introduction of artificial boundaries is not unique and thus, cannot be implemented easily into an automatic procedure.

The use of dual integral equations in crack problems was first reported by Bueckner [3]. In the boundary element method, dual integral equations were first presented by Watson [34], in a formulation based on the displacement equation and its normal derivative. The theoretical bases of the dual boundary element method were presented by Hong and Chen [15], in a general formulation which incorporates the displacement and the traction boundary integral equations. General crack problems can be solved with the dual boundary element method, when both the displacement and the traction boundary integral equations are simultaneously applied along the crack boundaries. Although the integration path is still the same for coincident points on the crack boundaries, the respective boundary integral equations are now distinct. Dual integral equations have been applied to solve problems in three-dimensional potential theory by Gray [9], and in three-dimensional elastostatics by Gray, Martha and Ingraffea [10]. An essential ingredient of both these formulations is the analytic evaluation of the hypersingular integrals over flat elements. This feature, which limits their analysis to the use of flat elements, requires non-standard boundary element interpolation functions for the integrations around the collocation node. Furthermore, the extension to edge crack problems was not dealt with in their analysis. Dual integral equations have also been applied to two-dimensional problems. In elastostatics Watson [34] presented a formulation limited to embedded cracks. In potential theory Rudolphi, Krishnasamy, Schmerr and Rizzo [30] presented results exhibiting unexplained oscillations. Recentelly, an alternative crack modelling strategy that caters for the analysis of general embedded and edge crack problems with the dual boundary element method, was presented by Portela, Aliabadi and Rooke [28]. In this formulation, both crack boundaries are discretized with discontinuous quadratic boundary elements. This results in a practical advantage because the problem of collocation at crack tips, crack kinks and crack-edge corners is automatically circumvented.

Within the limits of the linear elastic analysis, the stress field is unbounded at the tip of a crack. If r denotes the distance from the crack-tip, the stress field is of the order $r^{-1/2}$ and becomes singular as r tends to zero. The stress intensity factors,

defined at the crack-tip, are a measure of the strength of this singularity and play a fundamental role in linear elastic fracture mechanics. The techniques used in the dual boundary element method for the evaluation of stress intensity factors are described by Portela [27]. The J-integral technique, used in the present work, is based on a path-independent integral, Rice [29]. A simple procedure, based on the decomposition of the elastic field into its respective symmetric and antisymmetric mode components, is used to decouple the stress intensity factors of a mixed-mode problem.

The present work is concerned with the formulation and numerical implementation of the two-dimensional dual boundary element method, for the solution of general linear elastic crack problems. The dual boundary integral equations are presented in Section 2, and the crack modelling is discussed in Section 3. It is shown that the discretization of the crack boundaries is best done with discontinuous quadratic boundary elements. The effective treatment of the improper integrals of the dual equations, a matter of crucial importance in the dual boundary element method, is dealt with in Section 4. For curved boundary elements, the natural definition of ordinary finite-part integrals can be applied to regularize the improper integrals. For straight boundary elements, analytic integration is carried out. In Section 5 the J-integral is presented. The decoupling of the stress intensity factors into mode I and mode II components is implemented in the dual boundary element method in a straightforward manner; around each crack tip, a circular contour path is defined through a set of internal points located symmetrically with respect to the crack plane. Section 6 presents numerical results obtained for several edge and internal cracked geometries. The accuracy of the J-integral is shown with the edge and centre crack problems, as well as with a kinked crack problem. Finally, Section 7 presents the discussion and conclusions of the present work.

Throughout this work the Cartesian tensor notation is used and Einstein's summation convention is assumed.

2. The Dual Boundary Integral Equations

The dual boundary element method allows the analysis of general crack problems to be performed in a single-region analysis. The dual equations, on which the method is based, are the displacement and the traction boundary integral equations. In the absence of body forces, the boundary integral representation of the displacement components u_i, at an internal source point $\mathbf{x}^{'}$, is given by

$$u_i(\mathbf{x}^{'}) + \int_{\Gamma} T_{ij}(\mathbf{x}^{'}, \mathbf{x})\; u_j(\mathbf{x})\; d\Gamma(\mathbf{x}) = \int_{\Gamma} U_{ij}(\mathbf{x}^{'}, \mathbf{x})\; t_j(\mathbf{x})\; d\Gamma(\mathbf{x}), \tag{1}$$

where $T_{ij}(\mathbf{x}^{'}, \mathbf{x})$ and $U_{ij}(\mathbf{x}^{'}, \mathbf{x})$ represent the Kelvin traction and displacement fundamental solutions, respectively, at a field point $\mathbf{x}$ on the boundary Γ. The distance between the source point and the current field point is denoted by r and given by $|\mathbf{x} - \mathbf{x}^{'}|$. Since for an internal source point $r \neq 0$, the integrals in equation (1) contain regular integrands. Consider now the limit transition of equation (1) when the source point tends to the boundary, such that $r \to 0$. This operation can be implemented by taking the source point to the boundary and augmenting the problem domain by a semicircular region, with boundary Γ_{ε}^{*} and radius ε, centered at the source point, as shown in Figure 1.

With this configuration, the whole boundary is divided into two parts, $\Gamma = (\Gamma - \Gamma_{\varepsilon}) + \Gamma_{\varepsilon}^{*}$, and the limit transition of equation (1) is now carried out with the

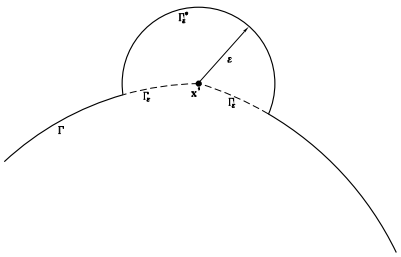

Figure 1. Source point located on the boundary, surrounded by a semicircular region.

parameter ε, in the form

$$u_i(\mathbf{x}^{'}) + \lim_{\varepsilon \to 0} \int_{\Gamma - \Gamma_\varepsilon + \Gamma_\varepsilon^*} T_{ij}(\mathbf{x}^{'}, \mathbf{x})\ u_j(\mathbf{x})\ d\Gamma(\mathbf{x}) = \lim_{\varepsilon \to 0} \int_{\Gamma - \Gamma_\varepsilon + \Gamma_\varepsilon^*} U_{ij}(\mathbf{x}^{'}, \mathbf{x})\ t_j(\mathbf{x})\ d\Gamma(\mathbf{x}). \qquad (2)$$

In equation (2), the right hand side integral contains a weakly singular integrand of order $\ln \frac{1}{r}$ and is integrable as an improper integral when the limit and the integration order are interchanged. The left hand side integral contains a strongly singular integrand of order $\frac{1}{r}$ and can be regularized with the first term of a Taylor's expansion of the displacements, about the source point, to give:

$$\begin{aligned} \lim_{\varepsilon \to 0} \int_{\Gamma - \Gamma_\varepsilon + \Gamma_\varepsilon^*} T_{ij}(\mathbf{x}^{'}, \mathbf{x})\ u_j(\mathbf{x})\ d\Gamma(\mathbf{x}) = & \lim_{\varepsilon \to 0} \int_{\Gamma_\varepsilon^*} T_{ij}(\mathbf{x}^{'}, \mathbf{x})\ [u_j(\mathbf{x}) - u_j(\mathbf{x}^{'})]\ d\Gamma(\mathbf{x}) + \\ & + u_j(\mathbf{x}^{'}) \lim_{\varepsilon \to 0} \int_{\Gamma_\varepsilon^*} T_{ij}(\mathbf{x}^{'}, \mathbf{x})\ d\Gamma(\mathbf{x}) + \\ & + \lim_{\varepsilon \to 0} \int_{\Gamma - \Gamma_\varepsilon} T_{ij}(\mathbf{x}^{'}, \mathbf{x})\ u_j(\mathbf{x})\ d\Gamma(\mathbf{x}). \end{aligned} \qquad (3)$$

Assuming that the displacements are Hölder continuous, that is there are constants $|C| < \infty$ and $0 < \alpha \leqslant 1$, such that the inequality

$$|u_j(\mathbf{x}) - u_j(\mathbf{x}^{'})| \leqslant C r^{\alpha}$$

holds, the first term of the right hand side of equation (3) is integrable and vanishes in the limiting process. The second limit expression of the right hand side of equation (3) leads to a jump on displacements, $A_{ij}(\mathbf{x}^{'})u_j(\mathbf{x}^{'})$, in which $A_{ij}(\mathbf{x}^{'})$ is a constant that depends on the local geometry and elastic constants. Finally, the third limit expression results in an improper integral that is taken in a Cauchy principal-value sense. Therefore, as $\varepsilon \to 0$ the source point tends to the boundary and, in the limit, equation (2) can be written in the form

$$c_{ij}(\mathbf{x}')u_j(\mathbf{x}^{'}) + \fint_{\Gamma} T_{ij}(\mathbf{x}^{'}, \mathbf{x})\ u_j(\mathbf{x})\ d\Gamma(\mathbf{x}) = \int_{\Gamma} U_{ij}(\mathbf{x}^{'}, \mathbf{x})\ t_j(\mathbf{x})\ d\Gamma(\mathbf{x}), \qquad (4)$$

where $\fint$ stands for the Cauchy principal-value integral and the coefficient $c_{ij}(\mathbf{x}^{'})$ is given by $\delta_{ij} + A_{ij}(\mathbf{x}^{'})$, in which δ_{ij} is the Kronecker delta.

At an internal source point $\mathbf{x}^{'}$, the stress components σ_{ij} are obtained by differentiation of equation (1) followed by the application of Hooke's law; they are given by

$$\sigma_{ij}(\mathbf{x}^{'}) + \int_{\Gamma} S_{ijk}(\mathbf{x}^{'},\mathbf{x})\; u_k(\mathbf{x})\; d\Gamma(\mathbf{x}) = \int_{\Gamma} D_{ijk}(\mathbf{x}^{'},\mathbf{x})\; t_k(\mathbf{x})\; d\Gamma(\mathbf{x}). \tag{5}$$

In this equation, $S_{ijk}(\mathbf{x}^{'},\mathbf{x})$ and $D_{ijk}(\mathbf{x}^{'},\mathbf{x})$ contain derivatives of $T_{ij}(\mathbf{x}^{'},\mathbf{x})$ and $U_{ij}(\mathbf{x}^{'},\mathbf{x})$, respectively. Since for an internal source point $r \neq 0$, the integrals in equation (5) contain regular integrands. Consider now the limit transition of equation (5) when the source point tends to the boundary, such that $r \to 0$. This operation can be performed exactly in the same way as for the displacement equation. Again, the whole boundary is divided into two parts, $\Gamma = (\Gamma - \Gamma_{\varepsilon}) + \Gamma^{*}_{\varepsilon}$, and the limit transition of equation (5) is now carried out with the parameter ε in the form

$$\sigma_{ij}(\mathbf{x}^{'}) + \lim_{\varepsilon\to 0} \int_{\Gamma-\Gamma_{\varepsilon}+\Gamma^{*}_{\varepsilon}} S_{ijk}(\mathbf{x}^{'},\mathbf{x})\; u_k(\mathbf{x})\; d\Gamma(\mathbf{x}) = \lim_{\varepsilon\to 0} \int_{\Gamma-\Gamma_{\varepsilon}+\Gamma^{*}_{\varepsilon}} D_{ijk}(\mathbf{x}^{'},\mathbf{x})\; t_k(\mathbf{x})\; d\Gamma(\mathbf{x}). \tag{6}$$

In this equation, the right hand side integral contains a strongly singular integrand of order $\frac{1}{r}$ and can be regularized with the first term of a Taylor's expansion of the tractions, about the source point, to give:

$$\begin{aligned}\lim_{\varepsilon\to 0} \int_{\Gamma-\Gamma_{\varepsilon}+\Gamma^{*}_{\varepsilon}} D_{ijk}(\mathbf{x}^{'},\mathbf{x})\; t_k(\mathbf{x})\; d\Gamma(\mathbf{x}) = &\lim_{\varepsilon\to 0} \int_{\Gamma^{*}_{\varepsilon}} D_{ijk}(\mathbf{x}^{'},\mathbf{x})\; [t_k(\mathbf{x}) - t_k(\mathbf{x}^{'})]\; d\Gamma(\mathbf{x}) + \\ &+ t_k(\mathbf{x}^{'}) \lim_{\varepsilon\to 0} \int_{\Gamma^{*}_{\varepsilon}} D_{ijk}(\mathbf{x}^{'},\mathbf{x})\; d\Gamma(\mathbf{x}) + \\ &+ \lim_{\varepsilon\to 0} \int_{\Gamma-\Gamma_{\varepsilon}} D_{ijk}(\mathbf{x}^{'},\mathbf{x}) t_k(\mathbf{x})\; d\Gamma(\mathbf{x}).\end{aligned} \tag{7}$$

Assuming Hölder-continuous tractions, the first term of the right hand side of equation (7) is integrable and vanishes in the limiting process. The second limit expression of the right hand side of equation (7) leads to a jump on tractions, given by $A_{ijk}(\mathbf{x}^{'})t_k(\mathbf{x}^{'})$, in which $A_{ijk}(\mathbf{x}^{'})$ is a constant that depends on elastic constants and coordinate transformations. The third limit expression in the right hand side of equation (7) results in an improper integral that is taken in a Cauchy principal-value sense. Consider now the left hand side integral of equation (6). It contains a hypersingular integrand of order $\frac{1}{r^2}$ that can be regularized with the first two terms of a Taylor's expansion of the displacements, about the source point, to give:

$$\lim_{\varepsilon\to 0}\int_{\Gamma-\Gamma_\varepsilon+\Gamma_\varepsilon^*} S_{ijk}(\mathbf{x}',\mathbf{x})\; u_k(\mathbf{x})\; d\Gamma(\mathbf{x}) = = \lim_{\varepsilon\to 0}\int_{\Gamma_\varepsilon^*} S_{ijk}(\mathbf{x}',\mathbf{x})\; [u_k(\mathbf{x}) - u_k(\mathbf{x}')$$
$$- u_{k,m}(\mathbf{x}')(x_m - x_m')]\; d\Gamma(\mathbf{x}) +$$
$$+ u_k(\mathbf{x}') \lim_{\varepsilon\to 0}\int_{\Gamma_\varepsilon^*} S_{ijk}(\mathbf{x}',\mathbf{x})\; d\Gamma(\mathbf{x}) + \qquad (8)$$
$$+ u_{k,m}(\mathbf{x}') \lim_{\varepsilon\to 0}\int_{\Gamma_\varepsilon^*} S_{ijk}(\mathbf{x}',\mathbf{x})(x_m - x_m')\; d\Gamma(\mathbf{x}) +$$
$$+ \lim_{\varepsilon\to 0}\int_{\Gamma-\Gamma_\varepsilon} S_{ijk}(\mathbf{x}',\mathbf{x}) u_k(\mathbf{x})\; d\Gamma(\mathbf{x}),$$

where the comma between two indices denotes differentiation. Assuming that the displacement derivatives are Hölder continuous, that is there are constants $|C| < \infty$ and $0 < \alpha \leqslant 1$, such that the inequality

$$|u_k(\mathbf{x}) - u_k(\mathbf{x}') - u_{k,m}(\mathbf{x}')(x_m - x_m')| \leqslant C|x_m - x_m'|^{\alpha+1}$$

holds, the first term of the right hand side of equation (8) is integrable and vanishes in the limiting process. The second limit expression in the right hand side of the same equation is unbounded and will be considered later. The third limit expression leads to a jump on displacement derivatives, given by $B_{ijkm}(\mathbf{x}')u_{k,m}(\mathbf{x}')$, in which $B_{ijkm}(\mathbf{x}')$ is a constant that depends on elastic constants and coordinate transformations. Finally, the fourth limit expression of the right hand side of equation (8) results in an improper integral. It can be shown that when this expression is taken together with the second limit expression, the result is always bounded [11]. Therefore, the fourth limit expression is considered alone, in a Hadamard [13] principal-value sense. Collecting the results of equations (7) and (8), it can be shown that for a source point in a smooth boundary the jump terms are equivalent to boundary stresses, that is

$$A_{ijk}(\mathbf{x}')t_k(\mathbf{x}') - B_{ijkm}(\mathbf{x}')u_{k,m}(\mathbf{x}') = \frac{1}{2}\sigma_{ij}(\mathbf{x}'). \qquad (9)$$

Therefore, as $\epsilon \to 0$, the source point tends to the boundary and, in the limit, on a smooth boundary, equation (6) can be written in the form

$$\frac{1}{2}\sigma_{ij}(\mathbf{x}') + \oint\!\!\!\!\!\!-_{\Gamma}\; S_{ijk}(\mathbf{x}',\mathbf{x})\; u_k(\mathbf{x})\; d\Gamma(\mathbf{x}) = \oint\!\!\!\!\!\!-_{\Gamma} D_{ijk}(\mathbf{x}',\mathbf{x})\; t_k(\mathbf{x})\; d\Gamma(\mathbf{x}), \qquad (10)$$

where $\oint\!\!\!\!\!\!-$ stands for the Hadamard principal value integral. Notice that equation (10) could be obtained by direct differentiation of equation (4), followed by the application of Hooke's law, when the relationship between Cauchy and Hadamard principal-value integrals is applied.

The traction components t_j are given by

$$\frac{1}{2}t_j(\mathbf{x}') + n_i(\mathbf{x}')\oint\!\!\!\!\!\!-_{\Gamma} S_{ijk}(\mathbf{x}',\mathbf{x})u_k(\mathbf{x})d\Gamma(\mathbf{x}) = n_i(\mathbf{x}')\oint\!\!\!\!\!\!-_{\Gamma} D_{ijk}(\mathbf{x}',\mathbf{x})t_k(\mathbf{x})d\Gamma(\mathbf{x}), \qquad (11)$$

where n_i denotes the i component of the unit outward normal to the boundary, at the source point. Equations (4) and (11) constitute the basis of the dual bound-

ary element method. A more complete description of the dual boundary element method is given by Portela [27].

3. Crack Modelling

The necessary conditions for the existence of the principal-value integrals obtained in the derivation of the dual boundary integral equations impose special restrictions on the crack modelling. Consider that both the geometry and boundary field variables are described by a piece-wise continuously differentiable approximation. Consider, further that collocation is always performed with the source point at the boundary element nodes. Under these considerations, the continuity requirements of Cauchy principal-value integral in the displacement equation can be satisfied by any Lagrangian continuous or discontinuous boundary element, since the shape functions imply a continuous displacement approximation at the nodes. However, in the traction equation the continuity requirements of the Hadamard principal-value integral are satisfied only by discontinuous elements, since all the nodes are internal points of the element where a continuously differentiable approximation is defined. Moreover, the requirement of the smoothness of the geometry at a collocation point in the traction equation is implicitly satisfied by the discontinuous element. Furthermore, discontinuous traction fields can be implicitly modelled by discontinuous elements, since the tractions must satisfy Hölder continuity only at the nodes. It is important to realize that if the element approximation does not satisfy these necessary continuity requirements then the principal value integrals do not exist.

For the sake of efficiency and to keep the simplicity of the standard boundary elements, the present formulation uses discontinuous quadratic elements for the crack modelling, as shown in Figure 2.

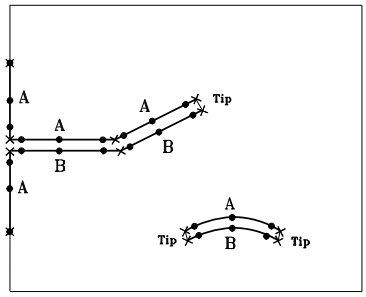

Figure 2. Crack modelling with discontinuous quadratic boundary elements.

The general modelling strategy, developed by Portela, Aliabadi and Rooke [28], can be summarized as follows:

- The traction equation (11) is applied for collocation on one of the crack boundaries.

- The displacement equation (4) is applied for collocation on the opposite crack boundary and remaining boundaries.
- The crack boundaries are discretized with discontinuous quadratic elements, as shown in Figure 2.
- Continuous quadratic boundary elements are used for discretization along the remaining boundaries of the problem domain, except at the intersection between a crack and an edge, where discontinuous or semi-discontinuous elements are required, in order to avoid nodes at the intersection.

This simple strategy is robust and allows the dual boundary element method to effectively model general edge or embedded crack problems; crack tips, crack-edge corners and crack kinks do not require special treatment, since they are not located at nodal points where the collocation is carried out. Other alternatives to discontinuous elements can be used to model the crack, but they are not as efficient. For instance, Hermitian boundary elements, Watson [34], and Overhouser boundary elements, Walters, Ortiz, Gibson and Bewer [33], also suit the continuity requirements. However, they are computationally expensive and are not readily suitable to deal with edge crack problems.

4. Computation of Principal-Value Integrals

The numerical implementation of the principal-value integrals that arise in the dual integral equations is easily carried out by the classical method of singularity subtraction, which leads to the natural definition of ordinary finite-part integrals. In the vicinity of a collocation node, the regular part of the integrand is expressed as a Taylor's expansion. If a sufficient number of terms of the expansion are subtracted from the regular part of the integrand and then separately added back, the singularity can be isolated. The original improper integral is thus transformed into the sum of a regular integral and an integral of the singular function. This latter integral is then evaluated analytically, while standard Gaussian quadrature is used for numerical integration of the regular integral. The procedure is general and applicable to any type of boundary element.

4.1 *General-Shape Discontinuous Elements*

On a traction-free crack, consider a discontinuous quadratic boundary element of general shape Γ_e that contains the collocation node. On this element, equations (4) and (11) become

$$c_{ij}(\mathbf{x}^{'})u_j(\mathbf{x}^{'}) + \oint\!\!\!\!\!\!-_{\Gamma_e} T_{ij}(\mathbf{x}^{'},\mathbf{x})\; u_j(\mathbf{x})\; d\Gamma(\mathbf{x}) = 0 \tag{12}$$

and

$$n_i(\mathbf{x}^{'}) \oint\!\!\!\!\!\!=_{\Gamma_e} S_{ijk}(\mathbf{x}^{'},\mathbf{x})u_k(\mathbf{x})d\Gamma(\mathbf{x}) = 0, \tag{13}$$

respectively. Coincident with this element, consider also a continuous quadratic boundary element which will be used for approximation of the local geometry. For both elements the local parametric coordinate ξ is defined, as usual, in the range $-1 \leqslant \xi \leqslant +1$. The collocation node $\xi^{'}$ is mapped onto $\mathbf{x}^{'}$, via the continuous element shape functions, while the displacement components u_j are approximated in

the local coordinate system by means of the nodal values u_j^n and the discontinuous element shape functions. The Cauchy principal value integral of equation (12) can be expressed in the local coordinate as

$$\int\!\!\!\!\!\!-_{\Gamma_e} T_{ij}(\mathbf{x}^{'},\mathbf{x})\; u_j(\mathbf{x})\; d\Gamma(\mathbf{x}) = u_j^n \int\!\!\!\!\!\!-_{-1}^{+1} \frac{f_{ij}^n(\xi)}{\xi-\xi^{'}}\; d\xi, \tag{14}$$

where $f_{ij}^n(\xi)$ is a regular function, given by the product of the fundamental solution, a shape function and the Jacobian of the coordinate transformation, multiplied by the term $\xi - \xi^{'}$. The integral of the right hand side of equation (14) can be transformed with the aid of the first term of a Taylor's expansion of the function f_{ij}^n, around the collocation node, to give

$$\int\!\!\!\!\!\!-_{-1}^{+1} \frac{f_{ij}^n(\xi)}{\xi-\xi^{'}}\; d\xi = \int_{-1}^{+1} \frac{f_{ij}^n(\xi) - f_{ij}^n(\xi^{'})}{\xi-\xi^{'}}\; d\xi + f_{ij}^n(\xi^{'}) \int\!\!\!\!\!\!-_{-1}^{+1} \frac{d\xi}{\xi-\xi^{'}}. \tag{15}$$

Now, the first integral of the right hand side is regular and the second one can be integrated analytically to give

$$\int\!\!\!\!\!\!-_{-1}^{+1} \frac{d\xi}{\xi-\xi^{'}} = \ln\left|\frac{1-\xi^{'}}{1+\xi^{'}}\right|. \tag{16}$$

In equation (15), the existence of the first-order finite-part integral requires the continuity of the first derivative of f_{ij}^n, or at least, the Hölder continuity of f_{ij}^n at the collocation node. For the discontinuous element, this requirement is automatically satisfied, because the nodes are internal points of the element, where f_{ij}^n is continuously differentiable.

The Hadamard principal value integral of equation (13) can be expressed in the local parametric coordinate as

$$\int\!\!\!\!\!\!=_{\Gamma_e} S_{ijk}(\mathbf{x}^{'},\mathbf{x})\; u_k(\mathbf{x})\; d\Gamma(\mathbf{x}) = u_k^n \int\!\!\!\!\!\!=_{-1}^{+1} \frac{g_{ijk}^n(\xi)}{(\xi-\xi^{'})^2}\; d\xi, \tag{17}$$

where $g_{ijk}^n(\xi)$ is a regular function, given by the product of the fundamental solution, a shape function and the Jacobian of the coordinate transformation, multiplied by the term $(\xi-\xi^{'})^2$. The integral of the right hand side of equation (17) can be transformed with the aid of the first and second terms of a Taylor's expansion of the function g_{ijk}^n, in the neighbourhood of the collocation node, to give

$$\begin{aligned}\int\!\!\!\!\!\!=_{-1}^{+1} \frac{g_{ijk}^n(\xi)}{(\xi-\xi^{'})^2}\; d\xi = &\int_{-1}^{+1} \frac{g_{ijk}^n(\xi) - g_{ijk}^n(\xi^{'}) - g_{ijk}^{n(1)}(\xi^{'})\,(\xi-\xi^{'})}{(\xi-\xi^{'})^2}\; d\xi + \\ &+ g_{ijk}^n(\xi') \int\!\!\!\!\!\!=_{-1}^{+1} \frac{d\xi}{(\xi-\xi^{'})^2} + \\ &+ g_{ijk}^{n(1)}(\xi^{'}) \int\!\!\!\!\!\!-_{-1}^{+1} \frac{d\xi}{\xi-\xi^{'}},\end{aligned} \tag{18}$$

where $g_{ijk}^{n(1)}$ denotes the first derivative. At the collocation node, the function g_{ijk}^n is required to have continuity of its second derivative or, at least, a Hölder-continuous first derivative, for the finite-part integrals to exist. This requirement is automatically satisfied by the discontinuous element, since the nodes are internal points of

the element. Now, in equation (18), the first integral of the right hand side is regular and the third integral is identical with the one given in equation (16). The second integral of the right hand side of equation (18) can be integrated analytically to give

$$\oint_{-1}^{+1} \frac{d\xi}{(\xi - \xi')^2} = -\frac{1}{1+\xi'} - \frac{1}{1-\xi'}. \tag{19}$$

Equations (15) and (18) are just the ordinary double-sided first and second order finite-part integrals, respectively, as defined by Kutt [19].

Numerical integration of singular integrands is also possible; quadrature rules for finite-part integrals were published by Ossicini [25], Kutt [20], Ioakimidis [16] and Ladopoulos [21].

4.2 *Straight Discontinuous Elements*

In many practical problems the cracks are straight; but cracks do grow along curved paths which are usually modelled as piece-wise straight. For piece-wise straight cracks, the integrals in equations (14) and (17) are carried out most effectively by direct analytic integration which is presented in the following. Consider a straight discontinuous quadratic boundary element, with the nodes positioned arbitrarily at the points $\xi = -\frac{2}{3}$, $\xi = 0$ and $\xi = +\frac{2}{3}$. The shape functions of this element are given by:

$$\begin{aligned} N_1 &= \xi\left(\frac{9}{8}\xi - \frac{3}{4}\right), \\ N_2 &= \left(1 - \frac{3}{2}\xi\right)\left(1 + \frac{3}{2}\xi\right), \\ N_3 &= \xi\left(\frac{9}{8}\xi + \frac{3}{4}\right). \end{aligned}$$

For this element, the integral of equation (14) is represented by:

$$\oint_{\Gamma_e} T_{ij}(\mathbf{x}', \mathbf{x})\; u_j(\mathbf{x})\; d\Gamma(\mathbf{x}) = u_j^n \oint_{-1}^{+1} T_{ij}(\xi', \mathbf{x}(\xi))\; N_n(\xi)\; J(\xi)\; d\xi = \mathbf{h}_i^n \mathbf{u}^n, \tag{20}$$

where $\mathbf{u}^n$ denotes the nodal displacement components and $J(\xi)$ is the Jacobian of the coordinate transformation. Because of the assumed straightness of the element, $J = \frac{l}{2}$, where l represents the element length and the matrix $\mathbf{h}^n$ is given by

$$\mathbf{h}^n = \frac{1-2\nu}{4\pi\,(1-\nu)} \begin{bmatrix} 0 & -1 \\ +1 & 0 \end{bmatrix} \oint_{-1}^{+1} \frac{N_n}{\xi - \xi'}\; d\xi. \tag{21}$$

The first order finite-part integrals are integrated analytically to give:

$$\oint_{-1}^{+1} \frac{N_1}{\xi - \xi'}\; d\xi = \frac{3}{4}\left(\frac{\xi'\left(3\xi' - 2\right)}{2} \ln\left|\frac{1-\xi'}{1+\xi'}\right| + 3\xi' - 2\right), \tag{22}$$

$$\oint_{-1}^{+1} \frac{N_2}{\xi - \xi^{'}}\, d\xi = \frac{1}{2}\left(\frac{\left(3\xi^{'} - 2\right)\left(3\xi^{'} + 2\right)}{2} \ln\left|\frac{1+\xi^{'}}{1-\xi^{'}}\right| - 9\xi^{'} \right) \tag{23}$$

and

$$\oint_{-1}^{+1} \frac{N_3}{\xi - \xi^{'}}\, d\xi = \frac{3}{4}\left(\frac{\xi^{'}\left(3\xi^{'} + 2\right)}{2} \ln\left|\frac{1-\xi^{'}}{1+\xi^{'}}\right| + 3\xi^{'} + 2 \right). \tag{24}$$

The integral of equation (17) is represented by

$$\oint_{\Gamma_e} S_{ijk}(\mathbf{x}^{'}, \mathbf{x})\, u_k(\mathbf{x})\, d\Gamma(\mathbf{x}) = u_k^n \oint_{-1}^{+1} S_{ijk}(\xi^{'}, \mathbf{x}(\xi))\, N_n(\xi)\, J(\xi)\, d\xi = \overline{\mathbf{h}}_{ij}^n \mathbf{u}^n, \tag{25}$$

where the matrix $\overline{\mathbf{h}}^n$ is given by:

$$\overline{\mathbf{h}}^n = \frac{E}{4\pi\left(1-\nu^2\right)} \frac{2}{l} \mathbf{S}^{'} \oint_{-1}^{+1} \frac{N_n}{\left(\xi - \xi^{'}\right)^2}\, d\xi. \tag{26}$$

The matrix $\mathbf{S}^{'}$ is given by

$$\mathbf{S}^{'} = \begin{bmatrix} +n_1(2n_2^2+1) & -n_2(-2n_2^2+1) \\ +n_1(2n_1^2-1) & -n_2(-2n_1^2-1) \\ -n_2(2n_1^2-1) & +n_1(-2n_2^2+1) \end{bmatrix}, \tag{27}$$

where n_1 and n_2 are the components of the unit outward normal to the element. The second-order finite-part integrals of equation (26) are integrated analytically to give:

$$\oint_{-1}^{+1} \frac{N_1}{(\xi - \xi^{'})^2}\, d\xi = \frac{3}{4}\left((3\xi^{'} - 1) \ln\left|\frac{1-\xi^{'}}{1+\xi^{'}}\right| + \frac{6\xi^{'2} - 2\xi^{'} - 3}{\xi^{'2} - 1} \right), \tag{28}$$

$$\oint_{-1}^{+1} \frac{N_2}{(\xi - \xi^{'})^2}\, d\xi = \frac{1}{2}\left(9\xi^{'} \ln\left|\frac{1+\xi^{'}}{1-\xi^{'}}\right| - \frac{18\xi^{'2} - 13}{\xi^{'2} - 1} \right) \tag{29}$$

and

$$\oint_{-1}^{+1} \frac{N_3}{(\xi - \xi^{'})^2}\, d\xi = \frac{3}{4}\left((3\xi^{'} + 1) \ln\left|\frac{1-\xi^{'}}{1+\xi^{'}}\right| + \frac{6\xi^{'2} + 2\xi^{'} - 3}{\xi^{'2} - 1} \right). \tag{30}$$

Equation (26) shows that the terms of the matrix $\overline{\mathbf{h}}^n$ are inversely proportional to the element length l. Notice that this property does not occur with the matrix $\mathbf{h}^n$ of equation (21).

4.3 *The Rigid Body Condition*

When collocation is performed at a crack node there are always two elements, on opposite faces, that contain the collocation point, because both crack boundaries are discretized. This means that, along the crack, the finite-part integrals in equations (12) and (13) are required twice: once on the element that contains the collocation node, that is the self-point element and again, on the opposite element, which is also a self-point element, since it contains the node which is coincident

with the collocation node. This peculiar feature of the dual boundary element method puts restrictions on the use of the rigid body condition at crack nodes, as explained in the following. Consider a constant displacement field, with components $u_i(\mathbf{x}) = C$, defined throughout the body. In this circumstance the traction components are zero and equation (4) gives

$$c_{ij}(\mathbf{x}^{'}) + \int_{\Gamma} T_{ij}(\mathbf{x}^{'}, \mathbf{x})\, d\Gamma(\mathbf{x}) = 0, \tag{31}$$

while equation (11) gives:

$$n_i(\mathbf{x}^{'}) \oint_{\Gamma} S_{ijk}(\mathbf{x}^{'}, \mathbf{x})\, d\Gamma(\mathbf{x}) = 0. \tag{32}$$

Equations (31) and (32) express the usual rigid body condition that must be satisfied by the dual boundary integral equations at every collocation point. According to equation (31), the coefficient $c_{ij}(\mathbf{x}^{'})$ need not be dealt with directly. When the equation is discretized, this coefficient, together with the finite-part integral, is determined by the *row sum* technique. However, for collocation at a crack node, the *row sum* technique can no longer be used if the integration along opposite self-point elements has any symmetric terms, since a pair of symmetric values always cancel each other in the sum. It can be shown, through equations (20) to (24), that the off-diagonal terms of the first and last nodes of the elements used here are symmetric, with the finite-part integrals given by $(\ln 5 - 3)$ and $(-\ln 5 + 3)$, respectively. Bearing in mind that opposite self-point elements have their first and last nodes interchanged, it is evident that two symmetric off-diagonal terms are obtained from the collocation at either one of these nodes and integration along opposite self-point elements. According to equation (32), it appears that the *row sum* technique can be used to evaluate indirectly the diagonal terms of the discretized form of the traction equation. Again, it can be shown, through equations (25) to (30), that the diagonal terms of any crack node are symmetric with respect to its opposite node. These features invalidate the use of the standard rigid body condition, to evaluate indirectly the diagonal terms at crack nodes.

5. The J–Integral Method

Consider a cartesian reference system, defined at the tip of a traction-free crack, as shown in Figure 3.

The J-integral is defined as

$$J = \int_{S} (\, W\, n_1 - t_j\, u_{j,1}\,)\, dS, \tag{33}$$

where S is an arbitrary contour surrounding the crack tip; W is the strain energy density; t_j are traction components and n_1 is the x-component of the unit outward normal to the contour path. The relationship between the J-integral and the stress intensity factors is given by

$$J = \frac{K_I^2 + K_{II}^2}{E^{'}}, \tag{34}$$

where $E^{'}$ is the elasticity modulus E for plane stress conditions and $E^{'} = E/(1-\nu^2)$

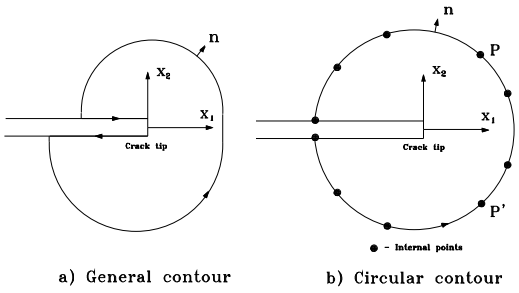

Figure 3. Coordinate reference system and contour path for J-integral.

for plane strain conditions.

In order to decouple the stress intensity factors in equation (34), the integral J is represented by the sum of two integrals as follows:

$$J = J^I + J^{II}, \tag{35}$$

where the superscripts indicate the deformation mode. For this representation to be possible, it is sufficient to decompose the displacement and stress fields into their symmetric and antisymmetric components, as described below. Consider two points, $P(x_1, x_2)$ and $P^{'}(x_1, -x_2)$, that are symmetric relative to the crack axis, as shown in Figure 3. At these points the displacement field can be expressed as a combination of symmetric and antisymmetric components in the form:

$$\left\{ \begin{array}{c} u_1 \\ u_2 \end{array} \right\} = \left\{ \begin{array}{c} +u_1^I + u_1^{II} \\ +u_2^I + u_2^{II} \end{array} \right\}, \quad \left\{ \begin{array}{c} u_1^{'} \\ u_2^{'} \end{array} \right\} = \left\{ \begin{array}{c} +u_1^I - u_1^{II} \\ -u_2^I + u_2^{II} \end{array} \right\}. \tag{36}$$

From equations (36), the symmetric and antisymmetric displacement components are given by:

$$\left\{ \begin{array}{c} u_1^I \\ u_2^I \end{array} \right\} = \frac{1}{2} \left\{ \begin{array}{c} u_1 + u_1^{'} \\ u_2 - u_2^{'} \end{array} \right\}, \quad \left\{ \begin{array}{c} u_1^{II} \\ u_2^{II} \end{array} \right\} = \frac{1}{2} \left\{ \begin{array}{c} u_1 - u_1^{'} \\ u_2 + u_2^{'} \end{array} \right\}. \tag{37}$$

At the same points $P(x_1, x_2)$ and $P^{'}(x_1, -x_2)$, the stress field can be expressed as a combination of symmetric and antisymmetric components in the form:

$$\left\{ \begin{array}{c} \sigma_{11} \\ \sigma_{22} \\ \sigma_{12} \end{array} \right\} = \left\{ \begin{array}{c} +\sigma_{11}^I + \sigma_{11}^{II} \\ +\sigma_{22}^I + \sigma_{22}^{II} \\ +\sigma_{12}^I + \sigma_{12}^{II} \end{array} \right\}, \quad \left\{ \begin{array}{c} \sigma_{11}^{'} \\ \sigma_{22}^{'} \\ \sigma_{12}^{'} \end{array} \right\} = \left\{ \begin{array}{c} +\sigma_{11}^I - \sigma_{11}^{II} \\ +\sigma_{22}^I - \sigma_{22}^{II} \\ -\sigma_{12}^I + \sigma_{12}^{II} \end{array} \right\}. \tag{38}$$

From equations (38), the symmetric and antisymmetric stress components are given by:

$$\left\{ \begin{array}{c} \sigma_{11}^I \\ \sigma_{22}^I \\ \sigma_{12}^I \end{array} \right\} = \frac{1}{2} \left\{ \begin{array}{c} \sigma_{11} + \sigma_{11}^{'} \\ \sigma_{22} + \sigma_{22}^{'} \\ \sigma_{12} - \sigma_{12}^{'} \end{array} \right\}, \quad \left\{ \begin{array}{c} \sigma_{11}^{II} \\ \sigma_{22}^{II} \\ \sigma_{12}^{II} \end{array} \right\} = \frac{1}{2} \left\{ \begin{array}{c} \sigma_{11} - \sigma_{11}^{'} \\ \sigma_{22} - \sigma_{22}^{'} \\ \sigma_{12} + \sigma_{12}^{'} \end{array} \right\}. \tag{39}$$

When equations (36) and (38) are introduced in equation (33), equation (35) is obtained, with the J-integral components given by

$$J^m = \int_S \left(W^m n_1 - t_j^m u_{j,1}^m \right) dS, \tag{40}$$

for $m = I$ or $m = II$. Finally, the following relationships hold:

$$J^I = \frac{K_I^2}{E'}, \quad J^{II} = \frac{K_{II}^2}{E'}. \tag{41}$$

The implementation of this procedure into the boundary element method is straightforward. A circular contour path, around the crack tip, is defined with a set of internal points, located at symmetrical positions, relative to the crack axis, as shown in Figure 3.

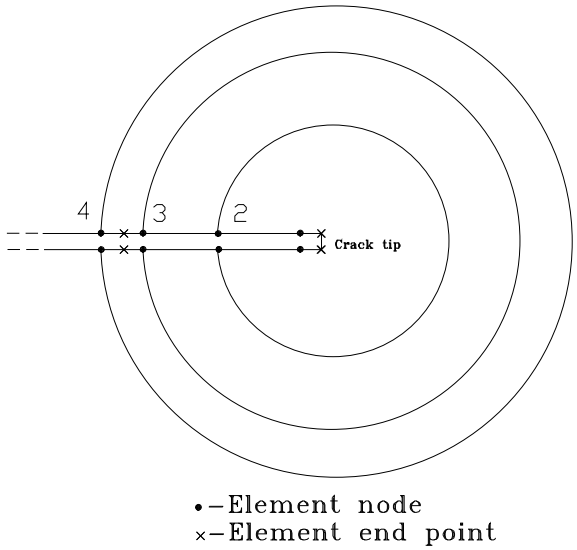

Figure 4. Circular path numbering system for J-integral contours.

The two contour points on the crack faces are the first and the last points of the path respectively. In a circular path, at these points it is always verified that $n_1 = -1$ and $n_2 = 0$ and thus, for a traction-free crack, $t_2 = 0$. The integration along the contour path can be accomplished with the trapezoidal or Simpson's rule or by Gaussian quadrature. For the sake of simplicity only circular paths, centered at the tip and containing a pair of crack nodes, were considered; each path is referred to by a path number which increases as the radius of the contour increases, see Figure 4.

6. Numerical Results

6.1 *The Edge Crack Problem*

Consider a square plate with a single edge crack, as represented in Figure 5. The crack length is denoted by a and the width of the plate is denoted by w. The plate is subjected to the action of a uniform traction $\bar{t}$, applied symmetrically at the ends in the direction perpendicular to the crack.

Results have been obtained and compared with those published by Civelek and Erdogan [4]. Five cases were considered, $a/w = 0.2$, 0.3, 0.4, 0.5 and 0.6. A convergence study was carried out with three different meshes of 32, 40, and 64 quadratic boundary elements, in which the crack was discretized with 4, 5 and 8 quadratic discontinuous elements on each surface.

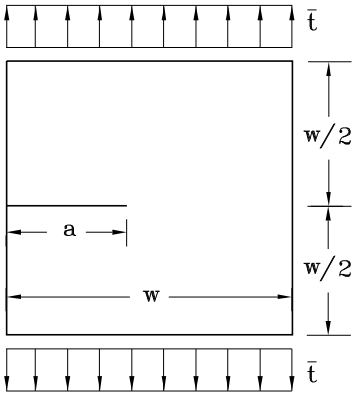

Figure 5. Square plate with a single edge crack.

The results, obtained with the mesh of 32 elements, in which the crack discretization was graded towards the tip with the ratios 0.4, 0.3, 0.2 and 0.1, are presented in Table 1.

Table 1. Stress intensity factors for a single edge crack in a square plate.

a/w	$K_I/\left(\bar{t}\sqrt{\pi a}\right)$					
	J-Integral Contour Path					Reference
	2	3	4	5	8	[4]
0.2	1.496	1.495	1.495	1.494	1.495	1.488
0.3	1.860	1.859	1.858	1.857	1.858	1.848
0.4	2.340	2.338	2.338	2.336	2.335	2.324
0.5	3.032	3.029	3.028	3.025	3.021	3.010
0.6	4.188	4.185	4.184	4.179	4.168	4.152

They show a high level of accuracy when compared with those of reference [4].

For the J-integral computations, 10 internal points and the trapezoidal rule were considered. The stability of the J-integral results, for any contour path, is noticeable.

6.2 *The Centre Crack Problem*

Consider, now, the analysis of a central slant crack in a rectangular plate, represented in Figure 6.

The ratio between the height and the width of the plate is given by $h/w = 2$. The crack has a length $2a$ and makes an angle of $\varphi = 45^\circ$ with the direction perpendicular to the applied traction. The plate is loaded with a uniform traction $\bar{t}$, applied symmetrically at the ends.

To solve this problem, a mesh of 36 quadratic boundary elements was set up, in which 6 discontinuous elements were used on each face of the crack, graded from the centre towards the tips, with the ratios 0.25, 0.15 and 0.1. Accurate results for this problem were published by Murakami [24]. The results obtained, presented in

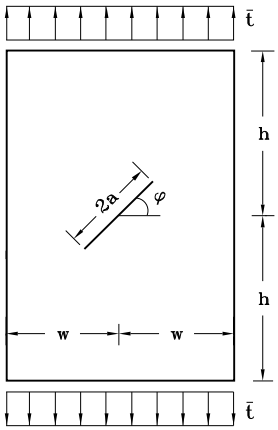

Figure 6. Rectangular plate with a central slant crack ($h/w = 2,\ \varphi = 45°$).

Table 2. Mode I stress intensity factors for a central slant crack in a rectangular plate ($h/w = 2,\ \varphi = 45°$).

a/w	$K_I/\left(\bar{t}\sqrt{\pi a}\right)$ J-Integral Contour Path					Reference
	2	3	4	5	8	[24]
0.2	0.521	0.519	0.521	0.521	0.521	0.518
0.3	0.544	0.542	0.544	0.544	0.544	0.541
0.4	0.575	0.574	0.576	0.576	0.576	0.572
0.5	0.616	0.614	0.617	0.617	0.616	0.612
0.6	0.666	0.665	0.667	0.667	0.666	0.661

Table 3. Mode II stress intensity factors for a central slant crack in a rectangular plate ($h/w = 2,\ \varphi = 45°$).

a/w	$K_{II}/\left(\bar{t}\sqrt{\pi a}\right)$ J-Integral Contour Path					Reference
	2	3	4	5	8	[24]
0.2	0.499	0.499	0.501	0.503	0.508	0.507
0.3	0.508	0.508	0.511	0.512	0.517	0.516
0.4	0.521	0.521	0.523	0.525	0.529	0.529
0.5	0.538	0.538	0.541	0.542	0.547	0.546
0.6	0.560	0.560	0.562	0.564	0.569	0.567

Tables 2 and 3, show an excellent accuracy when compared with the results of the reference [24].

The J-integral computations were carried out with 30 internal points and the trapezoidal integration rule. With such a coarse mesh, the results obtained are remarkably accurate. For mode II, the stability of the J-integral results is slightly lower than for mode I. This means that, in the deformation mode II, the variation of the elastic field along the contour paths is not properly approximated with the trapezoidal integration rule. Improved stability could be obtained by considering either more internal points along each path or a higher order integration rule.

6.3 *The General Crack Problem*

As a final test consider the analysis of a rectangular plate with an internal kinked crack, represented in Figure 8.

The ratio between the height and the width of the plate is given by $h/w = 2$. The segment of the crack of length a makes an angle of 90° with the direction of the applied traction, while the other segment makes an angle of 45° with the same

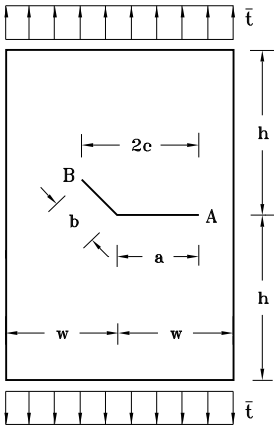

Figure 7. Rectangular plate with an internal kinked crack ($h/w = 2$, $a/w = 0.1$).

Table 4. Mode I stress intensity factors for tip A; rectangular plate with an internal kinked crack ($h/w = 2$, $a/w = 0.1$).

b/a	$K_I/\left(\bar{t}\sqrt{\pi c}\right)$ J-Integral Contour Path					Reference
	2	3	4	5	8	[24]
0.2	0.998	0.995	0.997	0.996	0.993	0.995
0.4	0.993	0.990	0.992	0.991	0.989	0.990
0.6	0.990	0.987	0.989	0.988	0.987	0.986

Table 5. Mode II stress intensity factors for tip A; rectangular plate with an internal kinked crack ($h/w = 2$, $a/w = 0.1$).

b/a	$K_{II}/\left(\bar{t}\sqrt{\pi c}\right)$ J-Integral Contour Path					Reference
	2	3	4	5	8	[24]
0.2	0.029	0.029	0.030	0.030	0.030	0.028
0.4	0.034	0.035	0.035	0.035	0.036	0.033
0.6	0.031	0.032	0.032	0.032	0.032	0.030

Table 6. Mode I stress intensity factors for tip B; rectangular plate with an internal kinked crack ($h/w = 2$, $a/w = 0.1$).

b/a	$K_I/\left(\bar{t}\sqrt{\pi c}\right)$ J-Integral Contour Path					Reference
	2	3	4	5	8	[24]
0.2	0.605	0.603	0.603	0.604	0.604	0.598
0.4	0.578	0.576	0.576	0.576	0.576	0.574
0.6	0.572	0.570	0.570	0.570	0.570	0.568

direction and has a length b. The projection of the total crack in the direction perpendicular to the traction is given by $2c = a + b/\sqrt{2}$. The kink of the crack is at the center of the plate which is loaded with a uniform traction $\bar{t}$, symmetrically applied at the ends of the plate. Three cases were considered, $b/a = 0.2$, 0.4 and 0.6, with $a/w = 0.1$. The stress intensity factors were obtained for both tips A and B with a boundary element mesh of 48 quadratic elements. The crack segment of length a was discretized with 5 discontinuous quadratic elements, on each crack face, while the other crack segment was discretized with 4 discontinuous quadratic elements on each crack face. Accurate results for comparison are published by Murakami [24]. The results of the stress intensity factors obtained for this problem, presented in Tables 4 to 7, are in excellent agreement with those of the reference [24]; even with the present relatively coarse mesh, the difference in the results is always less than

Table 7. Mode II stress intensity factors for tip B; rectangular plate with an internal kinked crack ($h/w = 2$, $a/w = 0.1$).

b/a	$K_{II}/\left(\bar{t}\sqrt{\pi c}\right)$ J-Integral Contour Path					Reference
	2	3	4	5	8	[24]
0.2	0.556	0.556	0.555	0.555	0.556	0.557
0.4	0.602	0.602	0.601	0.602	0.603	0.607
0.6	0.623	0.623	0.623	0.623	0.624	0.627

0.5%.

7. Discussion and Conclusions

The dual boundary element method incorporates two independent equations; one is the displacement boundary integral equation and the other one is the traction boundary integral equation. When the displacement equation is applied for collocation on one of the crack boundaries and the traction equation is applied for collocation on the other, general crack problems can be solved in a single-region formulation. Because of the continuity requirements imposed by the principal value integrals of the traction equation, both crack boundaries are discretized with discontinuous quadratic boundary elements. In addition, the discontinuous elements circumvent the problem of collocation at crack tips, crack kinks and crack-edge corners. The effective treatment of the hypersingular integrals that appear in the traction equation is of fundamental importance. For curved boundary elements, the natural definition of ordinary finite-part integrals is proposed in the present work. For straight boundary elements, the direct analytic integration is the most effective method to deal with such integrations. At a crack node, singular integrations occur twice, once on the self-point element and again on the opposite one. This feature prevents the use of the standard rigid body condition to evaluate indirectly the diagonal terms at crack nodes. Several cracked geometries were analyzed with the dual boundary element method. It was demonstrated that the dual boundary element method can be used for solving general crack problems efficiently.

A procedure based on the decomposition of the elastic field into its respective symmetric and antisymmetric components was used to decouple the stress intensity factors of mixed-mode problems. This procedure is implemented efficiently in the boundary element method because the integration path is defined with internal points, where the elastic field is accurately determined. This facility is not shared by the domain methods, like the finite element method, where the field variation is pre-assumed.

The reliability of the present modelling strategy, for the solution of general mixed-mode crack problems, was assessed with the analysis of standard benchmark problems. The accuracy of the J-integral was shown with the edge and centre cracked plates. As a final test the J-integral was applied in the analysis of a kinked-crack plate. The accuracy as well as the stability of the results, for any contour path, was excellent. In general, the J-integral was found to be an accurate tool for the stress intensity factor evaluation, in the analysis of crack problems with the dual boundary element method.

References

[1] Blandford, G.E., Ingraffea, A.R., Liggett, J.A., Two-Dimensional Stress Intensity Factor Computations Using the Boundary Element Method, Int. Journ. Num. Meth. Engng., **17** (1981) 387-404.

[2] Brebbia, C.A., Dominguez, J., Boundary Elements - an Introductory Course, Computational Mechanics Publications, Southampton, UK, (1989).
[3] Bueckner, H.F., Field Singularities and Related Integral Representations, Mechanics of Fracture (Ed. G.C. Sih), Volume 1, Nordhoff, (1973).
[4] Civelek, M.B., Erdogan, F., Crack Problems for a Rectangular Sheet and an Infinite Strip, Int. Journ. Frac., **19** (1982) 139-159.
[5] Courant, R., Hilbert, D., Methods of Mathematical Physics, Interscience Publishers, John Whiley, (1962).
[6] Crouch, S.L., Solution of Plane Elasticity Problems by the Displacement Discontinuity Method, Int. Journ. Num. Meth. Engng., **10** (1976) 301-342.
[7] Cruse, T.A., Boundary Element Analysis in Computational Fracture Mechanics, Kluwer Academic Publishers, (1989).
[8] Davis, P.J., Rabinowitz, P., Methods of Numerical Integration, Academic Press, (1984).
[9] Gray, L.J., Boundary Element Method for Regions with Thin Internal Cavities, IBM Bergen Scientific Centre, Allegaten 36, 5007 Bergen, Norway, (1987).
[10] Gray, L.J., Martha, L.F., Ingraffea, A.R., Hypersingular Integrals in Boundary Element Fracture Analysis, Int. Journ. Num. Meth. Engng., **29** (1990) 1135-1158.
[11] Guiggiani, M., Krishnasamy, G., Rizzo, F.J., Rudolphi, T.J., Hypersingular Boundary Integral Equations: A New Approach to Their Numerical Treatment, Proceedings of IABEM-90, Symposium of the International Association for Boundary Element Methods, University of Rome, Rome, Italy, October, (1990) 15-18.
[12] Guiggiani, M., Casalini, P., Direct Computation of Cauchy Principal Value Integrals in Advanced Boundary Elements, Int. Journ. Num. Meth. Engng., **24** (1987) 1711-1720.
[13] Hadamard, J., Lectures on Cauchy's Problem in Linear Partial Differential Equations, New Haven, Yale University Press, (1923).
[14] Hadamard, J., Lectures on Cauchy's Problem in Linear Partial Differential Equations, New Haven, Yale University Press, (1923).
[15] Hong, H., Chen, J., Derivations of Integral Equations of Elasticity, Journ. Engng. Mech., **114(6)** (1988) 1028-1044.
[16] Ioakimidis, N.I., On the Numerical Evaluation of Derivatives of Cauchy Principal-Value Integrals, Computing, **27** (1981) 81-88.
[17] Ioakimidis, N.I., Mangler-Type Principal Value Integrals in Hypersingular Integral Equations for Crack Problems in Plane Elasticity, Engng. Frac. Mech., **31** (1988) 895-898.
[18] Krishnasamy, G., Rudolphi, T.J., Schmerr, L.W., Rizzo F.J., Discretization Considerations with Hypersingular Integral Formulas for Crack Problems, in Discretization Methods in Structural Mechanics, G. Kuhn and H. Mang (Editors), Spinger–Verlag, (1990).
[19] Kutt H.R., On the Numerical Evaluation of Finite-Part Integrals Involving an Algebraic Singularity, CSIR Special Report WISK 179, National Research Institute for Mathematical Sciences, P. O. Box 395, Pretoria 0001, South Africa, (1975).
[20] Kutt, H.R., Quadrature Formulae for Finite-Part Integrals, Special Report WISK 178, National Research Institute for Mathematical Sciences, Pretoria, South Africa, (1975). Available also from the National Technical Information Service, U.S.A..
[21] Ladopoulos, E.G., On the Numerical Evaluation of the General Type of Finite-Part Singular Integrals and Integral Equations Used in Fracture Mechanics, Engng. Frac. Mech., **31(2)** (1988) 315-337.
[22] Linz, D.P., On the Approximate Computation of Certain Strongly Singular Integrals, Computing, **35** (1985) 345-353.
[23] Martin, P.A., Rizzo, F.J., On Boundary Integral Equations for Crack Problems, Proc. Roy. Soc., **A421** (1989) 341-355.
[24] Murakami, Y., Stress Intensity Factors Handbook, Pergamon Press, (1987).
[25] Ossicini, A., Alcune Formule di Quadratura per il Calcolo della Parte Finita e del Valore Principale di Integrali Divergenti, Rend. Matem., Ser. VI, **2** (1969) 385-401.
[26] Portela, A., Theoretical Basis of Boundary Solutions for Linear Theory of Structures, in New Developments in the Boundary Element Method, C.A.Brebbia (Editor), Proc. of the Second International Seminar on Recent Advances in Boundary Element Methods, University of Southampton, (1980).
[27] Portela, A., Boundary Elements in Crack Growth Analysis, Computational Mechanics Publications, Southampton, (1992).
[28] Portela, A., Aliabadi, M.H., Rooke, D.P., The Dual Boundary Element Method: Effective Implementation for Crack Problems, Int. Journ. Num. Meth. Engng., (to be published).
[29] Rice, J.R., A Path Independent Integral and the Approximate Analysis of Strain Concentration by Notches and Cracks, Trans. ASME, J. Appl. Mech., **35** (1968) 379-386.
[30] Rudolphi, T.J., Krishnasamy, G., Schmerr, L.W., Rizzo, F.J., On the Use of Strongly Singular Integral Equations for Crack Problems, Proc. Boundary Elements X, Computational Mechanics, Southampton, (1988).
[31] Sladek, V., Sladek, J., Balas, J., Boundary Integral Formulation of Crack Problems, ZAMM, **66** (1986) 83-94,.
[32] Snyder, M.D., and Cruse, T.A., Boundary Integral Equation Analysis of Cracked Anisotropic Plates, Int. Journal of Fracture, **11** (1975) 315-328.
[33] Walters, H.G., Ortiz, J.C., Gipson, G.S., Brewer, J.A., Overhouser Boundary Elements in Potential Theory and Linear Elastostatics, in Advanced Boundary Element Methods, T. A. Cruse (Editor), Springer Verlag, (1988).
[34] Watson, J.O., Hermitian Cubic Boundary Elements for the Analysis of Cracks of Arbitrary Geometry, in Advanced Boundary Element Methods, T. A. Cruse (Editor), Springer Verlag, (1988).